

## REFERENCES

1. A. Tayebi, J.G. Pérez, E. García, I.G. Diego, and M.F.C. Pérez, Optimized design of a compact probe for accurate near field measurements, *IEEE Trans Antennas Propag* 59 (2011), 2429–2433.
2. L.J. Foged, A. Giacomini, and R. Morbidini, Dual polarized probe for wideband planar near field measurement applications, *Proceedings of the 5th European Conference on Antennas and Propagation*, 2011, pp. 3402–3406.
3. B. Li, Y.Z. Yin, W. Hu, Y. Ding, and Y. Zhao, Wideband dual-polarized patch antenna with low cross polarization and high isolation, *IEEE Antennas Wireless Propag Lett* 11 (2012), 427–430.
4. E.B. Joy, W.M. Leach, G.P. Rodrigue, and D.T. Paris, Applications of probe-compensated near-field measurements, *IEEE Trans Antennas Propag* 26 (1978), 379–389.
5. E. Martini, O. Breinbjerg, and S. Maci, Reduction of truncation errors in planar near-field aperture antenna measurements using the Gerchberg-Papoulis, *IEEE Trans Antennas Propag* 56 (2008), 3485–3493.
6. J.S. Row and Y.H. Chen, Wideband planar array with broad beamwidth and low cross polarization, *IEEE Trans Antennas Propag* 63 (2015), 4161–4165.

© 2016 Wiley Periodicals, Inc.

## CAVITY RING-DOWN TECHNIQUE FOR REMOTE SENSING

S. Silva, M.B. Marques, and O. Frazão

INESC TEC and Department of Physics and Astronomy, Faculty of Sciences at University of Porto, Rua Do Campo Alegre 687, Porto 4169-007, Portugal; Corresponding author: sfsilva@inesctec.pt

Received 29 March 2016

**ABSTRACT:** This work demonstrates the viability of using a cavity ring-down (CRD) technique for remote sensing. A conventional CRD configuration is used where an optical circulator is added inside the fiber loop to couple 19 km of optical fiber with a gold mirror at its end with the purpose of remote sensing. As a proof-of-concept, an intensity sensor based on an eight-figure configuration is used at the end of the 19 km of fiber for displacement sensing. © 2016 Wiley Periodicals, Inc. *Microwave Opt Technol Lett* 58:2711–2713, 2016; View this article online at [wileyonlinelibrary.com](http://wileyonlinelibrary.com). DOI 10.1002/mop.30147

**Key words:** cavity ring down; optical fiber sensors; intensity sensors; displacement; remote sensing

### 1. INTRODUCTION

The optical time domain reflectometer (OTDR) was one of the first equipment to be used for remote sensing. The OTDR is a commercial device widely used for measuring losses along several kilometers of optical fiber, by detecting the loss of the Rayleigh backscattered light [1]. Early it was shown to be a promising device in measuring point-by-point losses, by using intensity sensors along the fiber. Several works have been reported in this area of research, where an OTDR is used to monitor sensors such as fiber Bragg gratings (FBGs) [2], long period gratings (LPGs) [3], multimode interference [4], fiber loop mirrors [5], and others. One of the main advantages is the quasi-distributed monitoring along 100 km of fiber without the use of amplification [1]. Currently, optical fiber sensors for remote sensing rely on nonlinear effects [6]. However, one of the main disadvantages of this type of configuration is the use of expensive equipment.

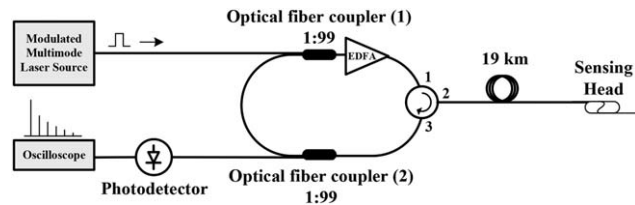


**Figure 1** Schematic of the CRD configuration developed for remote sensing. [Color figure can be viewed in the online issue, which is available at [wileyonlinelibrary.com](http://wileyonlinelibrary.com).]

Cavity ring down (CRD) is a well-known technique for monitoring intensity sensors and relies on the measurement of the decay time of an impulse travelling inside a fiber ring [7]. One of the main advantages of the conventional CRD technique is that the ring-down time is independent of the input power.

In this work, it is intended to demonstrate the viability of using a CRD technique for remote sensing. As a proof-of-concept, an intensity sensor with an eight-figure configuration is used at the end of several kilometers of optical fiber for the purpose of displacement sensing.

### 2. EXPERIMENTAL SETUP

The schematic of the CRD configuration proposed for remote sensing is presented in Figure 1. The basis of the fiber CRD configuration proposed for remote sensing relies on the operation principle of the conventional CRD technique as follows: a modulated multimode laser source (centered at 1550 nm) send pulses into a fiber loop, that is, the resonant cavity, which is formed by two optical fiber couplers with a 99:1 ratio. The two optical couplers operate analogue as the mirrors in a traditional bulk CRD. In the case of time resolved ring-down signals, the initially received intensity is very low, becoming even less with each round trip, due to the high split ratio of the optical couplers. However, the high reflectivity or coupling ratios are necessary to achieve large numbers of round trips (traveling more time inside the cavity). Therefore, the pulses enter into the fiber loop by means of 1% arm of the input coupler (1) and ring around inside the cavity. The amplitude of the pulses will slowly decay as it travels around the loop, due to losses in the fiber loop caused by fiber splices, insertion losses of the fiber couplers, and fiber intrinsic attenuation of 0.12 dB/m over 19 km (see Fig. 1).

Experimentally, the losses in the cavity were found to be very high so that the ring-down trace was not observable. To overcome this limitation, an Erbium Doped Fiber amplifier (EDFA) was inserted in the fiber loop (see Fig. 1) to provide an observable signal with a reasonable decay time. The EDFA was made in lab and comprises 2 m of an erbium-doped optical fiber with losses of 14 dB/m @ 980 nm. An amplification signal with 1.85 dB constant gain was applied to the several pulses traveling inside the cavity.

For the purpose of demonstrating remote sensing, an optical circulator was placed inside the fiber loop and connected to 19 km of optical fiber, whose end is coated with a gold thin film to form a high reflectivity mirror. Therefore, each pulse that enters in the cavity by means of 1% arm of the input coupler (1) is directed to the optical circulator (port 1), travels 19 km of optical fiber, and is back-reflected at the mirror, thus returning to the fiber loop (port 3 of the optical circulator). From here, the behavior is of a standard CRD, where the train of pulses rings around the fiber loop, with a decay rate given by

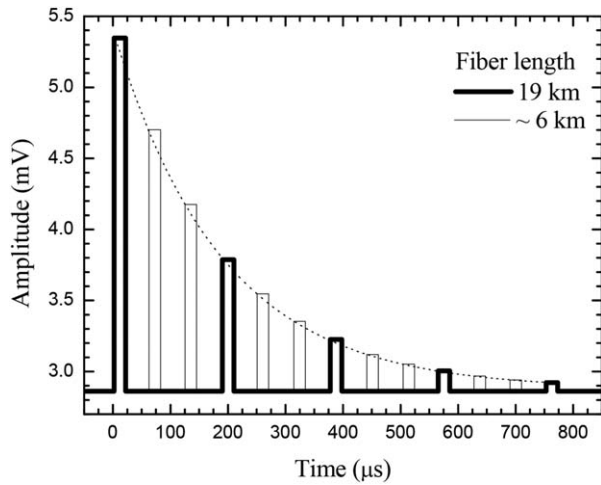


**Figure 2** Numerical analysis of the waveforms obtained for an input pulse with 20  $\mu\text{s}$  width and varying the fiber length. The bold trace is for 19 km of fiber and thin trace is for  $\sim 6$  km of fiber

the losses of the fiber-based system, being then coupled out via 1% arm of the output coupler (2). The output signal passes through a photodetector (gain of 40 dB) and the amplitude of the signal over time is monitored in an oscilloscope.

### 2.1. Numerical and Experimental Analysis of the Output Signal

A numerical analysis of the saturated waveform (input pulse with 20  $\mu\text{s}$  width) was performed. Figure 2 presents a simplified model concerning the saturated waveform for distinct fiber lengths used in the CRD configuration (bold line: 19 km, thin line:  $\sim 6$  km).

The pulse of the modulated multimode laser source is a well-defined square pulse with 20  $\mu\text{s}$  width. The numerical analysis relied on the sum of the several signals acquired by a typical pulse of the optical source and modulated by an exponential profile. The result was a series of square pulses with decreasing exponential amplitude, equally spaced by the time of a single round trip inside the fiber loop. This result is strongly dependent on the fiber length used. Therefore, the bold line in Figure 2 represents 19 km of fiber, while the thin line is for  $\sim 6$  km of fiber. This means that decreasing the fiber length, increases the

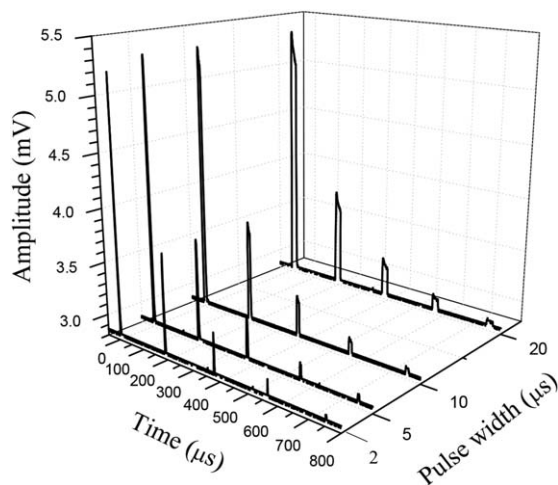


**Figure 3** CRD trace obtained for pulses sent by the modulated multimode laser source into the fiber loop with 20, 10, 5, and 2  $\mu\text{s}$  width

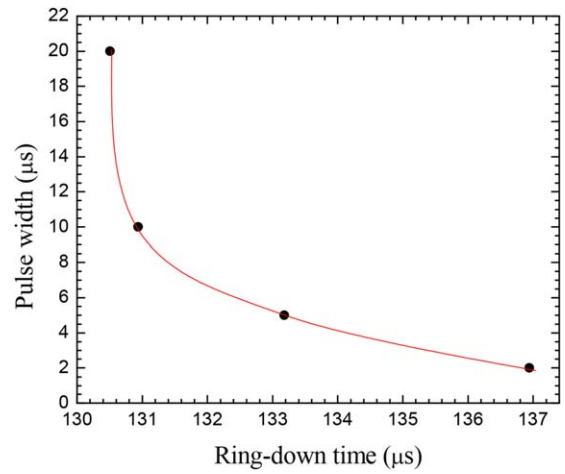


**Figure 4** Pulse width of the pulses sent by the modulated multimode laser source into the fiber loop versus the ring-down time of the waveforms obtained for each pulse width. [Color figure can be viewed in the online issue, which is available at [wileyonlinelibrary.com](http://wileyonlinelibrary.com).]

number of peaks observed. In this case, one can observe five peaks for 19 km of fiber while for  $\sim 6$  km of fiber thirteen peaks are observable. For this remote configuration, one may conclude that using more than 19 km of fiber becomes difficult to study precisely the time decay due to the small number of observable peaks.

In the proposed configuration, a modulated multimode laser source is used to send pulses down into the fiber loop. As the distance between pulses is large, it is possible to use a pulse width in the order of microseconds. However, the resulting waveform is strongly dependent on the pulse width, fiber length, fiber losses, and others. In this case, different pulse widths were studied (considering other parameters constant), namely, 20, 10, 5, and 2  $\mu\text{s}$ , and the resulting waveforms are depicted in Figure 3.

For a pulse width of 20  $\mu\text{s}$ , the output signal is saturated and five amplitude peaks are observed. This waveform has a ring-down time of about 130.5  $\mu\text{s}$ . The time for a single round trip is about 188  $\mu\text{s}$ , which corresponds to  $\sim 38.4$  km—this value was found by considering  $L = ct/n$ , where  $L$  is the fiber length of the configuration,  $c$  is the velocity of light and  $n$  is the core

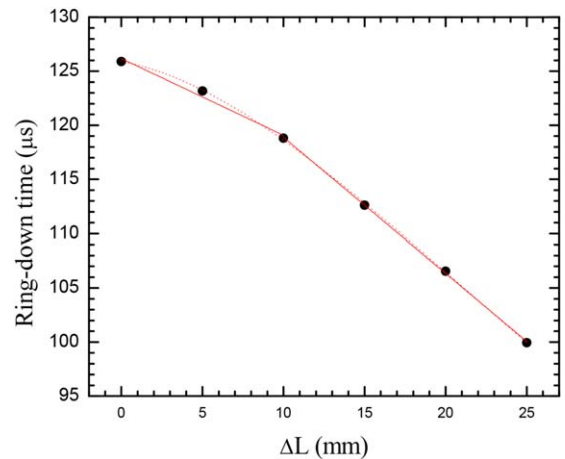


**Figure 5** Ring-down time versus displacement applied to the intensity-based sensor. [Color figure can be viewed in the online issue, which is available at [wileyonlinelibrary.com](http://wileyonlinelibrary.com).]

refractive index of the single-mode fiber used. Notice that, in this case, light travels 19 km of fiber as is back-reflected by the gold coating mirror, thus the effective travelled length is about 38 km. For this case, the numerical result is in a good agreement with the experimental value obtained.

For the waveform in Figure 3 obtained when a pulse width of  $2 \mu\text{s}$  is sent into the fiber loop, saturation of the signal is no longer observed. In this case, the waveform has a ring-down time of about  $136.9 \mu\text{s}$  and the time for a single round trip is  $188 \mu\text{s}$  (fiber length is the same). Because of the fiber length used in such configuration, the five observable peaks are better visualized in the case of signal saturation (pulse width of  $20 \mu\text{s}$ ).

Figure 4 presents the pulse width versus ring-down time obtained for the CRD configuration proposed for remote sensing. The nonlinear behavior results from the fact that less amplitude peaks are observable by decreasing pulse width, thus increasing the ring-down time of each waveform. Widening the input pulse will cause average amplification gain to decrease and, therefore, the decay time decreases as well.

## 2.2. Remote Sensing

To demonstrate the use of the proposed configuration for remote sensing, an intensity-based sensor was added to the CRD configuration to measure displacement. The sensing head was based on an eight-figure placed at the end of the 19 km of fiber and before the gold coating mirror. In practice, any other kind of intensity sensor may be used, such as LPGs, FBGs, fiber tapers, micromachined fibers, and others. In this approach, a pulse width of  $20 \mu\text{s}$  was used (see Fig. 3) to send pulses down into the fiber loop due to the possibility of better observing the five amplitude peaks.

To perform displacement ( $\Delta L$ ) measurements, the eight-figure was increasingly tightened (via sequential 5 mm steps) which corresponded to an increase of displacement. The result was the amplitude decrease of the output peaks when applying displacement to the sensor (i.e., tightening the eight-figure). The ring-down time for each waveform was measured and its variation as a function of displacement  $\Delta L$  is presented in Figure 5.

The observed behavior is due to the fact that tightening the eight-figure causes amplitude peaks to gradually decrease and disappear, thus, originating the ring-down time decrease with increasing displacement as well as the nonlinear behavior. Recall that, for the case of no displacement, the waveform is limited to only five peaks whose amplitude rapidly decreases for small variations of the intensity sensor. Maximum displacement was found to be at 25 mm, corresponding to a waveform with only three observable peaks. Afterwards, the ring-down time was not measurable. However, it is possible to measure displacement sensitivity in two distinct ranges. For the short range (0–10) mm, the sensitivity was found to be  $-0.71 \mu\text{s}/\text{mm}$ ; while for the long range (10–25) mm, the sensitivity is  $-1.25 \mu\text{s}/\text{mm}$ . One of the main advantages of using this remote sensing configuration is that the sensitivity of the sensing head placed before the mirror is two-fold when compared with the conventional CRD configuration where the sensing head is placed inside the fiber ring. This effect is expected due to light traveling twice the sensing head, which does not happen in the conventional CRD configuration [8].

## 3. CONCLUSION

Summarizing, it was demonstrated the viability of using CRD technique for remote sensing. A conventional CRD

configuration was developed where an optical circulator was added inside the fiber loop to couple 19 km of optical fiber with the purpose of remote sensing. The numerical analysis has shown to be in good agreement with the experimental result. An intensity sensor based on an eight-figure configuration was also used at the end of the 19 km of fiber to demonstrate the use of the proposed configuration for remote sensing.

## ACKNOWLEDGMENTS

This work was supported by Project “NORTE-01-0145-FEDER-000036,” which is financed by the North Portugal Regional Operational Programme (NORTE 2020), under the PORTUGAL 2020 Partnership Agreement, and through the European Regional Development Fund (ERDF). S.S. received a Pos-Doc fellowship (ref. SFRH/BPD/92418/2013) also funded by FCT—“Fundação para a Ciência e Tecnologia”.

## REFERENCES

1. M.P. Gold, A.H. Hartog, and D.N. Payne, A new approach to splice-loss monitoring using long-range OTDR, *Electron Lett* 20 (1984), 338–340.
2. S. Mendonça, O. Frazão, J.M. Baptista, and J.L. Santos, Fibre optic displacement sensing monitored by an OTDR and referenced by Fresnel reflection and by fibre Bragg gratings” *Microwave Opt Technol Lett* 49 (2007), 768–770.
3. O. Frazão, R. Falate, J.M. Baptista, J.L. Fabris, and J.L. Santos, Optical bend sensor based on a long-period fiber grating monitored by an OTDR, *Opt Eng* 44 (2005), 110502-1-3.
4. M.T.M.R. Giralddi, C.S. Fernandes, M.S. Ferreira, M.J. de Sousa, P. Jorge, J.C.W.A. Costa, J.L. Santos, and O. Frazão, Fiber optic displacement sensor based on a double-reflecting OTDR technique, *Microwave Opt Technol Lett* 57 (2015), 1312–1315.
5. M.T.M.R. Giralddi, C.S. Fernandes, M.S. Ferreira, M.J. de Sousa, P. Jorge, J.C.W.A. Costa, J.L. Santos, and O. Frazão, Fiber Loop Mirror Sensors Interrogated and Multiplexed by OTDR, *IEEE J Lightwave Technol* 33 (2015), 2580–2584.
6. J.P. Dakin, D.J. Pratt, G.W. Bibby, and J.N. Ross, Distributed Optical Fibre Raman Temperature Sensor Using A Semiconductor Light Source And Detector, *Electron Lett* 21 (1985), 569–570.
7. R.S. Brown, I. Kozin, Z. Tong, R.D. Oleschuk, and H.P. Looch, Fiber-loop ring-down spectroscopy, *J Chem Phys* 117 (2002), 10444–10447.
8. D.J. Passos, S.O. Silva, and O. Frazão, A New Cavity Ring-Down Topology for Remote Sensing, *Third Mediterranean Photonics Conference*, 7-9 May, Italy, 2014.

© 2016 Wiley Periodicals, Inc.

## AN ULTRA THIN POLARIZATION INSENSITIVE AND ANGULARLY STABLE MINIATURIZED FREQUENCY SELECTIVE SURFACE

**A.B. Varuna, Saptarshi Ghosh, and Kumar Vaibhav Srivastava**  
Department of Electrical Engineering, Indian Institute of Technology Kanpur, 208016, Uttar Pradesh, India; joysaptarshi@gmail.com

Received 30 March 2016

**ABSTRACT:** In this article, a novel polarization-insensitive and angularly stable miniaturized frequency selective surface (FSS) has been presented. The proposed structure has a single bandpass operation centred at 1.42 GHz, which is printed on an ultra-thin ( $0.00127\lambda_0$ ) dielectric substrate. Compared with earlier reported structures, the designed FSS demonstrates a better miniaturization performance having unit cell dimension of  $0.0378\lambda_0 \times 0.0378\lambda_0$ , where  $\lambda_0$  refers to free space